Atmos. Meas. Tech., 7, 1105–1119, 2014
www.atmos-meas-tech.net/7/1105/2014/
doi:10.5194/amt-7-1105-2014

Atmospheric Measurement Techniques
Open Access

The impact of spectral resolution on satellite retrieval accuracy of CO_2 and CH_4

A. Galli[1,2], S. Guerlet[3], A. Butz[4], I. Aben[1], H. Suto[5], A. Kuze[5], N. M. Deutscher[6,7], J. Notholt[6], D. Wunch[8], P. O. Wennberg[8], D. W. T. Griffith[7], O. Hasekamp[1], and J. Landgraf[1]

[1]SRON Netherlands Institute for Space Research, 3584 CA Utrecht, the Netherlands
[2]Physics Institute, University of Bern, 3012 Bern, Switzerland
[3]Laboratoire de Météorologie Dynamique, 75252 Paris, France
[4]Karlsruhe Institute of Technology, Institute for Meteorology and Climate Research, 76344 Leopoldshafen, Germany
[5]Japan Aerospace Exploration Agency, Tsukuba, Ibaraki 305-8505, Japan
[6]Institute of Environmental Physics, University of Bremen, 28334 Bremen, Germany
[7]Centre for Atmospheric Chemistry, University of Wollongong, Wollongong, NSW 2522, Australia
[8]Department of Earth Science and Engineering, California Institute of Technology, Pasadena, CA 91125, USA

Correspondence to: A. Galli (andre.galli@space.unibe.ch)

Received: 15 November 2013 – Published in Atmos. Meas. Tech. Discuss.: 4 December 2013
Revised: 26 February 2014 – Accepted: 13 March 2014 – Published: 29 April 2014

Abstract. The Fourier-transform spectrometer on board the Japanese GOSAT (Greenhouse gases Observing SATellite) satellite offers an excellent opportunity to study the impact of instrument resolution on retrieval accuracy of CO_2 and CH_4. This is relevant to further improve retrieval accuracy and to optimize the cost–benefit ratio of future satellite missions for the remote sensing of greenhouse gases. To address this question, we degrade GOSAT measurements with a spectral resolution of $\approx 0.24\,cm^{-1}$ step by step to a resolution of $1.5\,cm^{-1}$. We examine the results by comparing relative differences at various resolutions, by referring the results to reference values from the Total Carbon Column Observing Network (TCCON), and by calculating and inverting synthetic spectra for which the true CO_2 and CH_4 columns are known. The main impacts of degrading the spectral resolution are reproduced for all approaches based on GOSAT measurements; pure forward model errors identified with simulated measurements are much smaller.

For GOSAT spectra, the most notable effect on CO_2 retrieval accuracy is the increase of the standard deviation of retrieval errors from 0.7 to 1.0 % when the spectral resolution is reduced by a factor of six. The retrieval biases against atmospheric water abundance and air mass become stronger with decreasing resolution. The error scatter increase for CH_4 columns is less pronounced. The selective degradation of single spectral windows demonstrates that the retrieval accuracy of CO_2 and CH_4 is dominated by the spectral range where the absorption lines of the target molecule are located. For both GOSAT and synthetic measurements, retrieval accuracy decreases with lower spectral resolution for a given signal-to-noise ratio, suggesting increasing interference errors.

1 Introduction

Carbon dioxide (CO_2) and methane (CH_4) are the two most important anthropogenic greenhouse gases. Remote sensing of these gases with satellites allows us to globally monitor their atmospheric abundance. Both trace gases have to be retrieved with high accuracy to provide a significant contribution to our current knowledge of the Earth's climate system. Measurements of high spectral resolution are beneficial to reduce errors due to inaccurate spectroscopy and errors due to interfering retrieval species. However, good spatial coverage, high spatial resolution, and high signal-to-noise performance are competing requirements for satellite observations, which results in very expensive and complex instrument concepts. A careful trade-off between spectral resolution, spatial coverage, and cost has to be made. This study quantifies the

retrieval performance for reduced spectral resolution using the Greenhouse Gases Observing Satellite (GOSAT) observations in the 0.76 (O_2 A band), 1.6 (SWIR1a and SWIR1b), and 2.0 µm (SWIR2) spectral regions.

After the loss of the Envisat satellite in 2012 with the SCIAMACHY (SCanning Imaging Absorption spectroMeter for Atmospheric CHartographY) instrument (Bovensmann et al., 1999), the Japanese GOSAT satellite (Kuze et al., 2009) is currently the only satellite measuring total columns of greenhouse gases. In the next 2 years, NASA's OCO (Orbiting Carbon Observatory)-2 (Boesch et al., 2011) and the Chinese TanSat satellite (Liu et al., 2013) will join GOSAT to provide better coverage of satellite-based CO_2 measurements relevant to the climate research community. Meanwhile, the European Space Agency (ESA) is evaluating plans for the Carbon Monitoring Satellite (CarbonSat, Buchwitz et al., 2013) as one of two candidate Earth Explorer opportunity missions, scheduled for launch in 2018. Its goal is to monitor tropospheric CO_2 and CH_4 and to separate natural from anthropogenic greenhouse gas emissions by measuring reflected sunlight in the infrared. The next assured European space mission to observe both of these greenhouse gases, Sentinel-5, will follow after 2020 (Ingmann et al., 2012). It will not be optimized for CO_2 observations, though. Earth Explorer 8 will very likely be launched a few years after 2018. The intended spectral windows of OCO-2, TanSat, and CarbonSat are very similar to those of GOSAT: three separate spectral windows cover the O_2 A band at 0.765 µm, the weak CO_2 and CH_4 absorption lines at 1.6 µm, and the strong CO_2 absorption lines at 2.0 µm (see Table 1). The Fourier transform spectrometer on GOSAT has a full-width half-maximum (FWHM) resolution of 0.24 cm^{-1}, which is similar to OCO-2 (Boesch et al., 2011). The foreseen spectral resolution of TanSat lies between 0.25 and 0.5 cm^{-1} (Y. Liu, personal communication, 2013). CarbonSat is planned to operate at a resolution of 1.1–1.7 cm^{-1} in the near and shortwave infrared (Buchwitz et al., 2013). For Sentinel-5, a resolution of around 1.0 cm^{-1} is foreseen (Ingmann et al., 2012).

To cover the entire range of resolutions of the future satellite spectrometers, we considered in this study three spectral resolutions in addition to the GOSAT resolution: 0.5, 1.0, and 1.5 cm^{-1}. Because of the differing spectral windows, the study can only be indicative for some of the future missions. We prepared three data sets: GOSAT spectra collocated with TCCON observations, GOSAT spectra of 2 entire years over Europe, and a global ensemble of synthetic spectra. To degrade the spectral resolution of GOSAT measurements we convolved the spectra with a broad Gaussian or sinc function – equivalent to assuming a shorter optical path length for the GOSAT interferometer. No noise was added to the GOSAT spectra, i.e. we concentrate on the effect of the reduced spectral resolution and stick to the GOSAT signal-to-noise ratio (SNR). The question of whether a reduced retrieval performance at lower resolution can be compensated by a higher SNR can only be answered with synthetic data. We will briefly address this issue when we discuss the data set of simulated spectra.

The differences between retrieved greenhouse gas columns from GOSAT spectra and collocated TCCON observations served as our estimate for the absolute accuracy of GOSAT retrievals. The Total Carbon Column Observing Network (TCCON) is a global network of ground-based Fourier transform spectrometers, established in 2004 (Wunch et al., 2011a). Its goal is to remotely measure column abundances of CO_2, CO, CH_4, N_2O and other gases that absorb in the near-infrared (SWIR). Currently, there are 18 operational observation sites affiliated with TCCON. TCCON measurements are used to validate column abundances of greenhouse gases retrieved from satellite measurements (Butz et al., 2011; Morino et al., 2011; Parker et al., 2011; Wunch et al., 2011b; Reuter et al., 2011; Schepers et al., 2012; Oshchepkov et al., 2013; Guerlet et al., 2013).

The paper is structured as follows: in Sect. 2, we will describe the retrieval method, the GOSAT measurements, and the data selection. The results will be presented in Sect. 3. Section 3.1 covers the collocated GOSAT and TCCON data. In Sect. 3.2 we discuss the results for an approach where single spectral windows were spectrally degraded. Section 3.3 summarizes the results for the European data set, and Sect. 3.4 summarizes the results from synthetic retrievals. Section 4 will conclude the paper with recommendations for future satellite missions.

2 Data selection and retrieval method

2.1 Retrieval algorithm

To retrieve CO_2 and CH_4 from the GOSAT spectra, we used version 1.9 of the RemoTeC algorithm. The first version of the algorithm was described by Butz et al. (2011) in the context of GOSAT measurements and by Butz et al. (2010) in the context of synthetic spectra. The algorithm is based on the efficient radiative transfer model developed by Hasekamp and Butz (2008). From the measured radiances in one or several spectral windows, the algorithm simultaneously retrieves 12-layer profiles of CO_2 and CH_4 column densities along with other absorber species (water), surface albedo, spectral shifts, intensity offsets, and three effective aerosol parameters to describe the scattering properties of the atmosphere. The latter are the mean height of the scattering layer h_{aer}, the size parameter of the power-law distribution α_{aer}, and the total column number density of aerosols. Scattering particles are parametrized as spherical particles with a fixed refractive index ($1.400i \times 0.003$), and their size distribution follows a power law, $n(r) \sim r^{-\alpha_{\mathrm{aer}}}$, with r the particle radius. In the forward model, the aerosols exist in a single scattering layer with a Gaussian height distribution around the central height h_{aer}. Molecular absorption lines of O_2 and CO_2 are modelled by a spectroscopic model that includes

line mixing as well as collision-induced-absorption by O_2 (Tran and Hartmann, 2008; Lamouroux et al., 2010). Absorption by CH_4 and the interfering absorber H_2O is modelled by Voigt line-shape models based on HITRAN (high-resolution transmission) 2008 (Rothman et al., 2009). Since 2010, the RemoTeC algorithm has been improved in several ways. The version used for this study is described by Guerlet et al. (2013).

Total columns of CO_2 and CH_4 in units of molecules per square centimetre were the prime targets of the retrieval. After the retrieval converged, they were calculated as the sum of the retrieved absorber profile. When volume mixing ratios XCO_2 and XCH_4 were required (for comparison to TCCON values), the total columns were divided by the total dry air mass. The latter was not retrieved from the measurements; it was taken from values provided by the European Centre for Medium-Range Weather Forecasts (ECMWF). In this paper, we will always use volume mixing ratios to quantify retrieval accuracy.

GOSAT measurements with a cloud coverage larger than 5 % in the outer field of view were a priori rejected. This information is provided by the separate cloud and aerosol imager on board the GOSAT satellite. Apart from clouds, also low albedo or high scattering optical thickness can introduce systematic retrieval errors. To achieve a better retrieval accuracy, it is therefore necessary to filter the converged retrievals as well. Most inversions of GOSAT spectra converge to yield a result (80 % in the case of Europe from 2009 to 2011) but roughly half of these results should be excluded from further analysis because they are likely to exhibit large errors. Guerlet et al. (2013) experimented with different filters to selectively reject retrievals based on the retrieved parameters. In the present study, we adopted their most stringent a posteriori filter to quantify retrieval accuracy. The information required for this filter is supplied by the retrieval algorithm. No further model input or observations with different instruments (that may or may not be available for other satellite missions) is required. The filter operates independently for each spectral resolution. It reads

a. $\chi^2 / \mathrm{DFS} < 2 \times \mathrm{median}(\chi^2 / \mathrm{DFS})$

b. DFS of target species > 1.0

c. number of iterations < 11

d. $\sigma_{CO_2} < 0.3\,\%$, $\sigma_{CH_4} < 0.5\,\%$

e. $\tau_{\mathrm{aer}} < 0.25$

f. $3.0 < \alpha_{\mathrm{aer}} < 4.7$

g. $\tau_{\mathrm{aer}} h_{\mathrm{aer}} / \alpha_{\mathrm{aer}} < 300\,\mathrm{m}$

h. $-1 \times 10^{-9} <$ intensity offset at O_2 A band $< 7 \times 10^{-9}$

The filter makes use of fit residuals (χ^2 normalized by degrees of freedom), degrees of freedom for signal (DFS), number of iterations, relative precision of retrieved absorbers (σ_{CO_2} and σ_{CH_4}) derived from covariance matrix, retrieved aerosol optical thickness, retrieved aerosol load (τ_{aer} is the retrieved optical density at the O_2 A band, α_{aer} is the aerosol size parameter), and retrieved intensity offset. In case of a lowered resolution, the cut-off values for the precision (criterion d) are scaled by the worse average precision. The drawback of filtering the data in this manner is that the number of data points varies for runs at different spectral resolution. We therefore added a filter method for which the same retrievals were selected for every resolution at a given TCCON station (see Sect. 3.1).

GOSAT spectra affected by cirrus optical thickness (COT) larger than about 0.02 can be rejected a priori with the approach presented by Guerlet et al. (2013). For synthetic scenarios, the input COT was therefore reduced accordingly (see Sect. 3.4).

Table 1. Overview of spectral ranges used for inversion.

Description	Wavenumber range (cm^{-1})	Absorbing species
O_2 A band	12 920–13 195	O_2
SWIR1a	6170–6277.5	CO_2, H_2O, CH_4
SWIR1b	6045–6138	CH_4, H_2O, CO_2
SWIR2	4806–4896	CO_2, H_2O

2.2 GOSAT spectra and spectral degradation approaches

Table 1 summarizes the four spectral windows covered by GOSAT observations that are used by our retrieval algorithm. The spectral ranges will be kept fixed throughout the study.

The instrument line shapes (ILS) of the GOSAT spectra and of the two different degradation approaches are illustrated in Fig. 1. An example of a GOSAT spectrum (SWIR1a window from 6170 to 6277.5 cm^{-1}) at original (black line) and at 1.5 cm^{-1} resolution (red line) is shown in Fig. 2. The first approach consisted of convolving the GOSAT spectra with a Gaussian instrumental line shape of a FWHM broader than the original FWHM. The effective FWHM of the resulting ILS was then considered the spectral resolution of the degraded spectrum. The broader the FWHM of the convolution compared to the GOSAT ILS, the closer the new line shape resembles a Gaussian shape (see red line in Fig. 1). The retrieval is not limited to any specific line shape, since the forward model spectrum is subjected to the same convolution before it is compared to the degraded input spectrum. As an independent degradation approach, we truncated the original interferograms with a five-times smaller optical path distance than the default. This is mathematically equivalent to convolving the spectrogram with a sinc ILS (see dashed blue line in Fig. 1). The effective FWHM of the

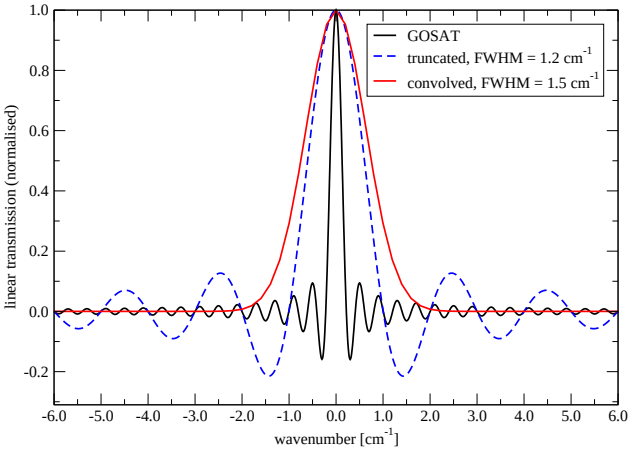

Fig. 1. Instrument line shapes for three different resolutions. Black line: GOSAT resolution, blue dashed line: truncated interferogram (effective FWHM = 1.2 cm^{-1}), and red line: GOSAT ILS convolved with a Gaussian distribution (effective FWHM = 1.5 cm^{-1}).

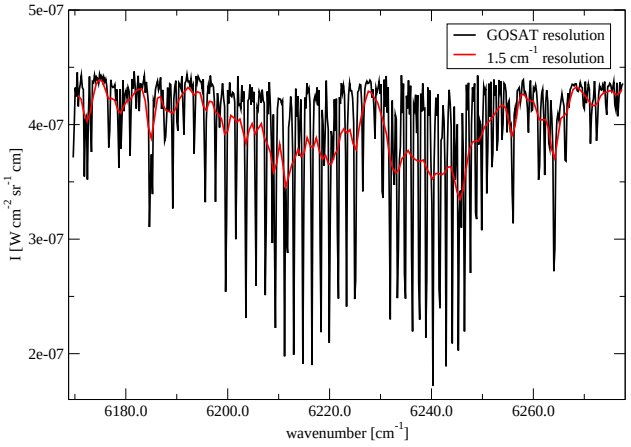

Fig. 2. Spectral intensity in the SWIR1a window, for GOSAT resolution (black) and for a spectrum convolved to FWHM = 1.5 cm^{-1} resolution (red).

truncation approach amounts to 1.2 cm^{-1}. For the convolution approach, the oversampling ratio was 2.5 for all windows, for the original GOSAT spectra and the truncation approach it was 1.0. Varying the oversampling ratio between 1.0 and 3.0 for the convolution approach did not notably affect the retrieval accuracy beside shifting the global bias (by 0.2 % at most).

The two approaches reflect different instrument concepts. Convolution with a Gaussian distribution emulates the instrument properties of a grating spectrometer as employed for OCO, Sentinel-5, and CarbonSat, whereas the truncated interferogram provides the spectral reflectance from a Fourier transform spectrometer. The second approach also allowed us to verify that the decrease in retrieval accuracy is driven by the spectral resolution and does not depend on the degradation method. After this verification, the first approach was chosen as default method for the rest of the study.

The measurement noise of the degraded spectra were deduced from the measurement noise of the original GOSAT measurement. No extra noise was added to the degraded spectra. The measurement uncertainty of each spectral point is needed at all resolutions to invert the spectra. For GOSAT spectra, the SNR is 300, defined under conditions of a diffusive reflectivity of 30 % at a solar zenith angle (SZA) of 30° (Kuze et al., 2009). The measurement uncertainty of the spectrum is derived from this SNR assuming a shot-noise-limited instrument model. The SNR of the degraded spectra is scaled from the original spectra by interpreting the convolution as a running average over the spectrum. This implies the same optical throughput of the instrument per pixel independent of the sampling. Since the absolute uncertainty of the original spectrum is almost constant against wavenumber, quadratic error propagation leads to

$$\sigma_{\mathrm{deg}} = \sigma \sqrt{\frac{\mathrm{FWHM}}{\mathrm{FWHM}_{\mathrm{deg}}}} \tag{1}$$

for the measurement uncertainty of the degraded spectrum. This ensures that the square sum of fit residuals as well as the precision of the retrieved CO_2 and CH_4 columns do not vary by more than a factor of two for all spectral resolutions. For the spectra generated from the truncated interferogram, the measurement error was estimated from GOSAT level-1 processing. From the measurement uncertainties, the typical relative precision of retrieved columns calculated to $\sigma_{CO_2} = 0.2\,\%$ and $\sigma_{CH_4} = 0.4\,\%$ for GOSAT resolution. For the lowest spectral resolution of 1.5 cm^{-1}, the precision decreased to $\sigma_{CO_2} = 0.3\,\%$ and $\sigma_{CH_4} = 0.6\,\%$. These values were only relevant for the a posteriori filter criteria. The systematic errors, assessed with TCCON measurements and simulations, usually exceeded the precision. In this manuscript we focus on systematic errors as this error source is the most relevant for the targeted application areas (e.g. Basu et al., 2013, and references therein). Systematic errors can be divided into smoothing errors, model parameter errors (e.g. spectroscopy errors), forward model errors due to the imperfect treatment of scatterers, and interference errors. This distinction follows Sussmann and Borsdorff (2007). They define interference as an error introduced by additional physical quantities that are retrieved together with the target species. The most prominent examples are other molecules, i.e. H_2O and CH_4 for a CO_2 retrieval. In measurements, interference errors of course coexist with other error sources but synthetic measurements allow disentangling some of them (see Sect. 3.4).

2.3 Selection of data sets

We prepared and evaluated three data sets for this study.

1. All GOSAT observations between April 2009 and May 2011 that are collocated in space and time (within $5^\circ \times 5^\circ$ and 2 hours) with ground-based observations of the TCCON network.

2. The same 25 months, but for all of Europe and northern Africa without TCCON reference values. This comprises roughly 12 000 GOSAT observations. We chose these regions for their high variability in solar zenith angle and albedo (including partly snow-covered scenes and desert).

3. An ensemble of 11 036 simulated GOSAT observations for all four seasons and for the entire land surface, set up by Butz et al. (2012).

In all three cases, we retrieved the column densities of CO_2 and CH_4 with our full-physics retrieval from the GOSAT spectra at the original resolution. Then, we degraded the spectra to lower resolutions of 0.5, 1.0, and 1.5 cm^{-1} and repeated the retrieval.

Elaborating on the first publication by Butz et al. (2011) on GOSAT retrievals with the RemoTeC algorithm, Guerlet et al. (2013) prepared sets of GOSAT data for 12 TCCON sites, spanning 2 years. The GOSAT data are collocated to TCCON measurements, i.e. they coincide with each other in space and time. The authors tested two different collocation criteria: the straight-forward spatio-temporal collocation required that a GOSAT measurement be sampled at a time within 2 hours of a TCCON measurement and at a geolocation less than 5° from the TCCON station. A more refined collocation criterion was based on a larger geolocation ($\pm 7.5^\circ$ in latitude and $\pm 22.5^\circ$ in longitude) box and model fields (Basu et al., 2013) of CO_2. Only those GOSAT data were kept for which the modelled XCO_2 is close to the modelled value at the TCCON station (less than 0.5 ppm difference). For the present study, we decided to apply the first collocation criterion as the second criterion depends critically on the CO_2 model fields and cannot be directly translated to a CH_4 collocation criterion. Furthermore, we concentrated on the six TCCON stations where we had more than 100 collocated measurements. These are the stations at Park Falls (USA), Lamont (USA), Orléans (France), Białystok (Poland), Darwin (Australia), and Wollongong (Australia). Our results can thus be compared to the previous publications by Guerlet et al. (2013) on CO_2 retrievals and by Schepers et al. (2012) on CH_4 retrievals.

The CO_2 and CH_4 columns observed with TCCON have been calibrated with other data sets (Wunch et al., 2010). We therefore considered them as the best available reference values. Nevertheless, relying only on comparisons at TCCON stations to check retrieval accuracy has a few drawbacks. First, TCCON stations are concentrated in the Northern Hemisphere and do not cover the entire range of relevant parameters, e.g. the ground albedo (Guerlet et al., 2013). Second, the statistics necessary for correlation studies and to assess inter-station biases are limited because only six TCCON stations offer a reasonably large amount of collocated TCCON and GOSAT observations since the start of GOSAT in 2009. Third, any definition of collocation is somewhat arbitrary (as discussed by Guerlet et al., 2013). Therefore, we also introduced data sets 2 and 3 and studied the relative changes of retrieved CO_2 and CH_4 for the whole European continent (offering many more data points) and the retrieval accuracy without spectroscopic errors for the case of synthetic data.

3 Results

This section provides the results for the different data sets defined in Sect. 2.3. We first present the comparison of GOSAT retrieval results and TCCON reference values for different spectral resolution (Sect. 3.1). This step also serves to verify that our results agree with previous work on GOSAT retrievals. We then proceed with two further approaches, degrading only single spectral windows (Sect. 3.2) and using a wider observation range without TCCON reference values (Sect. 3.3). Section 3.4 on synthetic spectra completes the results section.

3.1 Retrievals at TCCON stations

Following previous studies on GOSAT retrieval performance (Butz et al., 2011; Morino et al., 2011; Parker et al., 2011; Wunch et al., 2011b; Reuter et al., 2011; Schepers et al., 2012; Oshchepkov et al., 2013; Guerlet et al., 2013) we rely on results obtained at TCCON stations to assess retrieval accuracy in absolute terms. The main drawback for this approach is that only a small fraction of all GOSAT measurements can be used for such an assessment. We therefore check if the results observed at the six TCCON stations (Park Falls, Lamont, Orléans, Białystok, Darwin, and Wollongong) in this section can be reproduced when we extend the observations beyond TCCON locations (Sect. 3.3).

Tables 2 and 3 summarize the results for our nominal filter method (Guerlet et al., 2013) for CO_2 and CH_4, respectively. We used the same filter method as Guerlet et al. (2013) to compare our results to previous work. Because the filter criteria were identical at all spectral resolutions, the number of included retrievals varied with resolution. The number of converged retrievals (in total and also the fraction inside the filter) dropped by up to 25 % when the spectra were degraded from GOSAT resolution down to 1.5 cm^{-1}. This decrease is not a necessary consequence of lower spectral resolution since convergence rates depend on the assumed measurement uncertainty. The truncation approach with a FWHM of 1.2 cm^{-1} implies slightly larger measurement uncertainties. As a result, it yielded convergence rates similar to the original GOSAT retrievals. The varying number of retrievals may pose a problem for interpretation: any filter that reduces

Table 2. Retrieval performance for XCO_2 with respect to TCCON results, PF: Park Falls, LA: Lamont, OR: Orléans, BI: Białystok, DA: Darwin, WO: Wollongong. For each spectral resolution, the three rows denote from top to bottom: number of filtered retrievals, scatter, and bias. The bias and scatter are given as relative deviation from TCCON results in percentages %.

Station	PF	LA	OR	BI	DA	WO	**Total**
GOSAT	307	654	201	155	125	192	**1634**
(0.24 cm^{-1})	0.58	0.49	0.53	0.62	0.75	0.94	$\langle\sigma\rangle$ = **0.65**
	−0.64	−0.66	−0.76	−0.64	−0.41	−0.07	$\langle b\rangle$ = −0.53, σ_b = **0.22**
FWHM = 0.5 cm^{-1},	272	545	182	127	209	163	**1498**
convolution	0.62	0.55	0.65	0.75	0.69	0.99	$\langle\sigma\rangle$ = **0.71**
	−0.87	−0.88	−1.01	−0.87	−0.71	−0.33	$\langle b\rangle$ = −0.78, σ_b = **0.20**
FWHM = 1.0 cm^{-1},	258	521	166	115	124	156	**1340**
convolution	0.80	0.65	0.83	0.99	0.89	1.13	$\langle\sigma\rangle$ = **0.88**
	−0.59	−0.49	−0.75	−0.68	−0.3	+0.10	$\langle b\rangle$ = −0.46, σ_b = **0.27**
FWHM = 1.2 cm^{-1},	187	660	N/A	N/A	N/A	N/A	
truncation	0.88	0.76					
	−0.94	−0.67					
FWHM = 1.5 cm^{-1},	239	460	127	95	127	146	**1194**
convolution	0.94	0.69	0.91	1.05	1.01	1.23	$\langle\sigma\rangle$ = **0.97**
	−0.51	−0.21	−0.63	−0.55	−0.03	+0.26	$\langle b\rangle$ = −0.28, σ_b = **0.32**

Table 3. Retrieval performance for XCH_4 with respect to TCCON results. Same format as Table 2.

Station	PF	LA	OR	BI	DA	WO	**Total**
GOSAT	265	642	179	144	125	186	**1541**
(0.24 cm^{-1})	0.76	0.76	0.77	0.78	0.84	1.21	$\langle\sigma\rangle$ = **0.85**
	−0.33	−0.20	−0.43	−0.40	−0.43	−0.17	$\langle b\rangle$ = −0.33, σ_b = **0.11**
FWHM = 0.5 cm^{-1},	252	540	167	115	109	162	**1345**
convolution	0.80	0.80	0.92	0.80	0.77	1.25	$\langle\sigma\rangle$ = **0.89**
	−0.71	−0.55	−0.91	−0.98	−0.72	−0.67	$\langle b\rangle$ = −0.76, σ_b = **0.17**
FWHM = 1.0 cm^{-1},	267	520	152	106	124	159	**1328**
convolution	0.93	0.84	1.01	0.90	0.85	1.30	$\langle\sigma\rangle$ = **0.97**
	−0.69	−0.61	−1.09	−1.17	−0.60	−0.70	$\langle b\rangle$ = −0.81, σ_b = **0.27**
FWHM = 1.2 cm^{-1},	190	664	N/A	N/A	N/A	N/A	
truncation	0.90	0.80					
	−0.28	−0.44					
FWHM = 1.5 cm^{-1},	250	466	121	88	127	149	**1201**
convolution	1.00	0.94	1.21	0.92	0.89	1.23	$\langle\sigma\rangle$ = **1.03**
	−0.59	−0.44	−1.16	−1.19	−0.55	−0.60	$\langle b\rangle$ = −0.76, σ_b = **0.34**

the number of considered retrievals based on fit quality (e.g. residuals, precision, or amount of scatterers) excludes predominantly difficult retrievals with a larger error. By using tighter filter criteria, the error scatter of the remaining retrievals can thus be improved at the expense of number of retrievals. To compare the retrieval accuracy derived with two different algorithms or at different spectral resolutions, the number of included retrievals should always be the same. We therefore added Tables 4 and 5 for a more stringent filter. Here, we culled the filtered data sets to those retrievals that pass the criteria for all resolutions. This gives an unbiased impression on the relative performance degradation with spectral resolution.

Tables 2–5 list the retrieval performance for XCO_2 or XCH_4 for all six TCCON stations (columns) and for all spectral resolutions (rows). The three numbers in a cell indicate, from top to bottom, the number of converged retrievals inside the filter, the standard deviation of relative retrieval errors compared to TCCON reference values in percentage, and the median of the relative retrieval error in percentage.

The second number will be referred to as scatter σ, the last number will be referred to as bias b. The last column summarizes the performance for all six TCCON stations, indicating total number of retrievals, average scatter $\langle\sigma\rangle$, average bias $\langle b\rangle$, and the inter-station bias σ_b. The latter is the standard deviation of the six biases, weighted by the inverse of the scatter at each station.

The main effect of the lower resolution on XCO_2 accuracy is the increase in error scatter. It increases continuously with decreasing spectral resolution by a factor of 1.5 from GOSAT resolution to the 1.5 cm^{-1} resolution. This holds true for both data selection methods (last columns in Tables 2 and 4). The increase of the XCH_4 error scatter is more modest. For the filter method used by Guerlet et al. (2013), $\langle\sigma\rangle$ increased from 0.85 to 1.03 % (last column in Table 3), and for the reduced number of retrievals (Table 5), $\langle\sigma\rangle$ increased from 0.81 to 0.97 %. The average retrieval bias of XCO_2 changed in a seemingly random pattern by a few 0.1 %s for each step to lower resolution, whereas the inter-station bias σ_b hardly increased from typically 0.2 to 0.3 %. For XCH_4, the change in mean bias by -0.4 % appeared at all lower resolutions except for the truncation approach (but even here, a negative shift was observed).

The bias shift of CH_4 is reminiscent of the study by Galli et al. (2012) done for the 4190–4340 cm^{-1} spectral range. They showed that degrading TCCON spectra from a resolution of 0.02 to 0.45 cm^{-1} introduces a CH_4 retrieval bias of 0.5 %. The results in Tables 2 and 3 are also consistent with Petri et al. (2012), who compared the measurement accuracy of the TCCON interferometer to a lower resolution interferometer with a FWHM of 0.11 cm^{-1}. They found that reducing the resolution of TCCON spectra introduced an XCH_4 offset of 0.26 %, whereas it was negligible for XCO_2. The authors speculated that this dependence on spectral resolution is caused by inaccurate prior profiles and/or inaccurate spectroscopy of CH_4 or interfering gases. Moreover, Petri et al. (2012) estimated the error scatter of retrieved CO_2 and CH_4 columns from the daily standard deviation of individual measurements. It was larger for the lower-resolution spectrometer than for the TCCON-type of instrument. The relative increase amounted to a factor of 1.4 for XCO_2 and a factor of 1.9 for XCH_4. This increase is not identical to our results, since the spectral resolution, the retrieval ranges and the observation geometry (backscattered sunlight in contrast to the direct, ground-based solar observations considered by Petri et al., 2012, and Galli et al., 2012) differ. Nonetheless, substantially degrading the resolution of a spectrum seems to have the general effect of increasing the standard deviation of retrieval errors and of introducing bias shifts on the order of several 0.1 %s. Contrary to XCH_4, no general trend of XCO_2 biases with lower spectral resolution can be established.

For the collocation criterion used in our study, Guerlet et al. (2013) found (their Table 2, right column) $\langle b\rangle = -0.36$ % and $\langle\sigma\rangle = 0.65$ % (2.5 ppm) for 12 TCCON stations between April 2009 and December 2010 for XCO_2. This agrees well with the values in Table 2 of $\langle b\rangle = -0.53$ % and $\langle\sigma\rangle = 0.65$ %. The small change in bias is due to the TCCON reference values. In October 2012, an improved TCCON data release became available on http://tccon.ipac.caltech.edu/ (software version GGG2012 instead of GGG2009). In this paper we used these more recent values, whereas the values presented by Guerlet et al. (2013) refer to the older version GGG2009. The only notable difference between old and new TCCON results is a constant shift of XCO_2 by -0.125 %. Guerlet et al. (2013) derived an inter-station bias of 0.24 %, defined as standard deviation of the 12 biases weighted by the scatter at each station. In our study, the inter-station bias shows little sensitivity, increasing only from 0.22 to 0.32 % as spectral resolution decreases.

In contrast to Guerlet et al. (2013), Butz et al. (2011) also compared XCH_4 results of GOSAT retrievals to TCCON values. They used the same six TCCON stations as in this study but their database only extended to summer 2010, and their results were obtained with an older version of the RemoTeC software. Nevertheless, their mean scatter of 0.015 ppm (parts per million; 0.85 % relative error) and mean bias of -0.34 % agree well with our study ($\langle\sigma\rangle = 0.85$ % and $\langle b\rangle = -0.33$ % according to Table 3). The increase of inter-station bias with lower resolution is statistically significant at a 99.5 % confidence level for both data filtering methods (Tables 3 and 5). For a larger set of 12 TCCON stations, Schepers et al. (2012) found a larger (at GOSAT resolution) inter-station XCH_4 bias of $\sigma_b = 0.24$ %, whereas their $\langle\sigma\rangle = 0.95$ % and $\langle b\rangle = -0.37$ % are similar to this study.

The method of spectral degradation (i.e. convolution versus truncation) did not affect the retrieval performance: the error scatter of CO_2 and CH_4 columns for the truncation method (fourth row in Tables 4 and 5) fits well to the results for similar resolutions (third and fifth rows of same tables). The only change is seen in the global bias. We also examined if the correlation of retrieval errors with light path and atmospheric parameters are comparable if identical retrievals from Park Falls and Lamont are selected. For both CO_2 and CH_4, the dependency of retrievals on water, SZA, and albedo for the truncated interferograms followed exactly the trend set by the convolution retrievals at similar resolutions. This is demonstrated by Fig. 3 for the water dependency: over the range from 0 to 2×10^{23} H_2O molecules cm^{-2}, the XCO_2 retrieval error increases by 1.18 % for 1.0 cm^{-1}, 1.10 % for 1.2 cm^{-1}, and by 1.54 % for 1.5 cm^{-1} (the results for the convolution approach correspond to the blue curve in Fig. 4). For the rest of this work, we will therefore concentrate on the convolution approach.

To study the dependence of CO_2 and CH_4 retrieval errors on physical parameters, we calculated linear regressions of the retrieval differences (with respect to TCCON reference values) as a function of atmospheric water abundance, air mass, surface albedo at the SWIR1b window, retrieved aerosol optical thickness at the O_2 A band, and aerosol size parameter ($1/\alpha_{aer}$). The air mass of an observation is

Table 4. Retrieval performance for XCO_2 with respect to TCCON results, same format as Table 2, but the data were reduced to the identical retrievals for all resolutions.

Station	PF	LA	OR	BI	DA	WO	**Total**
GOSAT	117	364	108	80	92	105	**866**
(0.24 cm^{-1})	0.53	0.44	0.46	0.59	0.60	0.82	$\langle\sigma\rangle$ = **0.57**
	−0.70	−0.63	−0.82	−0.74	−0.43	−0.07	$\langle b\rangle$ = −0.57, σ_b = **0.24**
FWHM = 0.5 cm^{-1},	117	364	108	80	92	105	**866**
convolution	0.62	0.49	0.55	0.61	0.65	0.89	$\langle\sigma\rangle$ = **0.64**
	−0.97	−0.81	−1.12	−1.04	−0.72	−0.32	$\langle b\rangle$ = −0.83, σ_b = **0.25**
FWHM = 1.0 cm^{-1},	117	364	108	80	92	105	**866**
convolution	0.76	0.56	0.74	0.82	0.78	1.06	$\langle\sigma\rangle$ = **0.79**
	−0.67	−0.44	−0.75	−0.82	−0.21	+0.08	$\langle b\rangle$ = −0.47, σ_b = **0.31**
FWHM = 1.2 cm^{-1},	117	364	N/A	N/A	N/A	N/A	
truncation	0.79	0.60					
	−0.84	−0.62					
FWHM = 1.5 cm^{-1},	117	364	108	80	92	105	**866**
convolution	0.84	0.62	0.86	0.93	0.85	1.15	$\langle\sigma\rangle$ = **0.88**
	−0.55	−0.20	−0.55	−0.59	+0.08	+0.37	$\langle b\rangle$ = −0.24, σ_b = **0.36**

Table 5. Retrieval performance for XCH_4 with respect to TCCON results. Same format as Table 4.

Station	PF	LA	OR	BI	DA	WO	**Total**
GOSAT	102	363	98	72	92	106	**833**
(0.24 cm^{-1})	0.74	0.76	0.81	0.71	0.70	1.12	$\langle\sigma\rangle$ = **0.81**
	−0.14	−0.16	−0.46	−0.53	−0.46	−0.20	$\langle b\rangle$ = −0.33, σ_b = **0.19**
FWHM = 0.5 cm^{-1},	102	363	98	72	92	106	**833**
convolution	0.74	0.81	0.98	0.72	0.74	1.14	$\langle\sigma\rangle$ = **0.86**
	−0.64	−0.51	−1.03	−1.14	−0.75	−0.68	$\langle b\rangle$ = −0.79, σ_b = **0.26**
FWHM = 1.0 cm^{-1},	102	363	98	72	92	106	**833**
convolution	0.78	0.84	1.09	0.75	0.79	1.20	$\langle\sigma\rangle$ = **0.91**
	−0.57	−0.53	−1.15	−1.19	−0.60	−0.65	$\langle b\rangle$ = −0.78, σ_b = **0.32**
FWHM = 1.2 cm^{-1},	102	363	N/A	N/A	N/A	N/A	
truncation	0.79	0.80					
	−0.28	−0.45					
FWHM = 1.5 cm^{-1},	102	363	98	72	92	106	**833**
convolution	0.80	0.94	1.19	0.82	0.84	1.24	$\langle\sigma\rangle$ = **0.97**
	−0.53	−0.42	−1.20	−1.18	−0.53	−0.65	$\langle b\rangle$ = −0.75, σ_b = **0.36**

related to the SZA and the VZA (viewing zenith angle) via $1/\cos(\mathrm{SZA}) + 1/\cos(\mathrm{VZA})$. The retrieved aerosol size parameter strongly correlates with water and air mass of a retrieval scenario at any resolution. A dependency on those parameters will also lead to a dependency on α_{aer}. This is the reason why aerosol size is being used to a posteriori filter the data (Guerlet et al., 2013). This effect may be restricted to algorithms that retrieve scatterers with a few effective parameters and thus should not be interpreted as general consequence of a lowered spectral resolution. Figures 4 and 5 present the results as slope of the linear regressions ($\pm 1\sigma$-uncertainty) for the four different resolutions available at all six TCCON stations. If the slope is zero within its uncertainty, the retrieval error does not significantly depend on the corresponding parameter. An increase in the slope with decreasing resolution means that accuracy becomes worse as the retrieval errors correlate more strongly with physical parameters. All slopes were evaluated to span the maximum parameter range that can be encountered for GOSAT retrievals passing the a posteriori filter. These ranges are as follows: water – from 0 to 2×10^{23} molecules cm^{-2}, air mass – from 2.0 to 4.0, albedo – from 0.1 to 0.4, retrieved

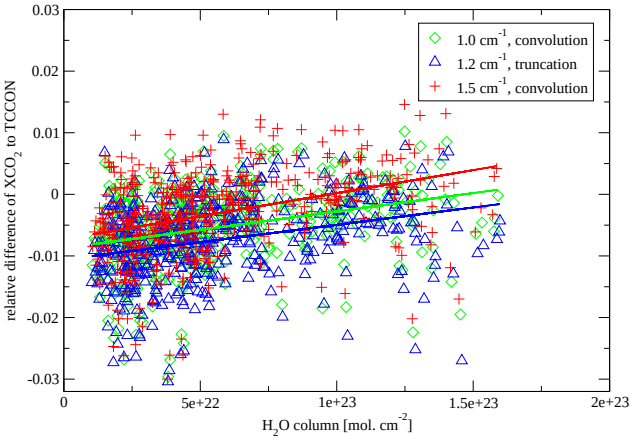

Fig. 3. Retrieval errors of XCO_2 as a function of water content of the atmosphere, identical filtered retrievals at Park Falls and Lamont for all three resolutions. The linear regressions of XCO_2 versus water are shown as straight lines: green (1.0 cm^{-1} convolution approach), blue (1.2 cm^{-1} truncation approach), and red (1.5 cm^{-1} convolution).

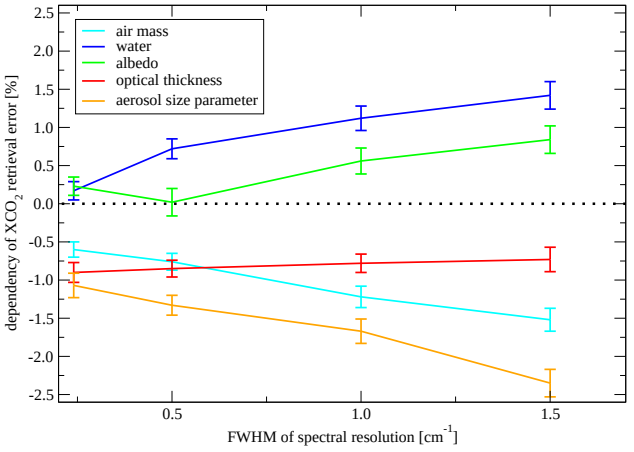

Fig. 4. Linear dependence of XCO_2 retrieval errors on physical parameters as a function of spectral resolution. Shown are the slopes of the linear regression of retrieval errors versus air mass (light blue), water abundance (dark blue), surface albedo at 1.6 µm (green), retrieved optical thickness at the O_2 A band (red), and the inverse of the aerosol size parameter (orange).

optical thickness – from 0 to 0.25, and inverse of the aerosol size parameter – from 1/4.7 to 1/3.0 (by definition of the a posteriori filter). In this way, slopes for different physical parameters can be directly compared to each other. Figures 4 and 5 demonstrate that CO_2 dependencies are generally more sensitive to spectral degradation than CH_4 dependencies. The only exception is the water dependency, which becomes more pronounced for both absorbers.

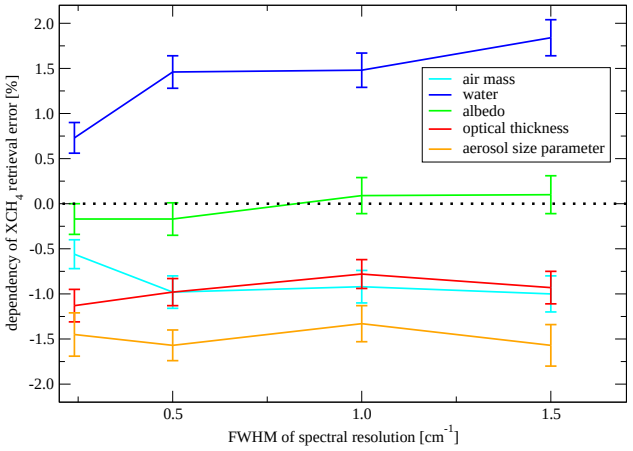

Fig. 5. Linear dependence of XCH_4 retrieval errors on physical parameters as a function of spectral resolution. Same format as Fig. 4.

3.2 Single-window degradation

To determine the spectral windows that are more severely affected by spectroscopic or interference errors, we also degraded single windows. We repeated the retrievals at the six TCCON stations degrading only one of the four retrieval windows to 1.5 cm^{-1} resolution. The results of this selective degradation are shown in Fig. 6. The upper panel shows the change of error scatter $\langle\sigma\rangle$ relative to the retrieval results at GOSAT resolution in all windows. The lower panel shows the absolute change in bias $\langle b\rangle$. The only retrievals used were those that passed the a posteriori filters for every spectral resolution scenario. The total number of filtered retrievals varied by up to 20 % for different scenarios and absorbers but no clear correlation with retrieval accuracy was visible.

For XCH_4, the picture is simple. Only when the SWIR1b window (6045–6138 cm^{-1}) was degraded, did the negative shift in bias and the increase in scatter occur. In that case also the dependency of retrieval error on water abundance became stronger whereas the dependency remained at the level found for original GOSAT resolution for the three other scenarios. This indicates that the CH_4 and H_2O spectroscopy in the 1.6 µm range might still benefit from improvements. For XCO_2, the bias most markedly increased when the SWIR1a window (6170–6277.5 cm^{-1}) was degraded, whereas the scatter increased to a similar extent when the SWIR1a or the SWIR2 window was degraded.

This reflects the position of CO_2 absorption lines in SWIR1a and SWIR2 and strong CH_4 absorption lines in SWIR1b (Rothman et al., 2009). In contrast, degrading the O_2 A window had a rather small effect on the retrieved columns. Our results imply that a degradation of the SWIR2 window does not affect XCH_4 retrieval accuracy because no CH_4 absorption lines are present. Aerosol parameters were apparently retrieved at a similar accuracy for the SWIR2 degradation scenario as for the non-degraded case, otherwise

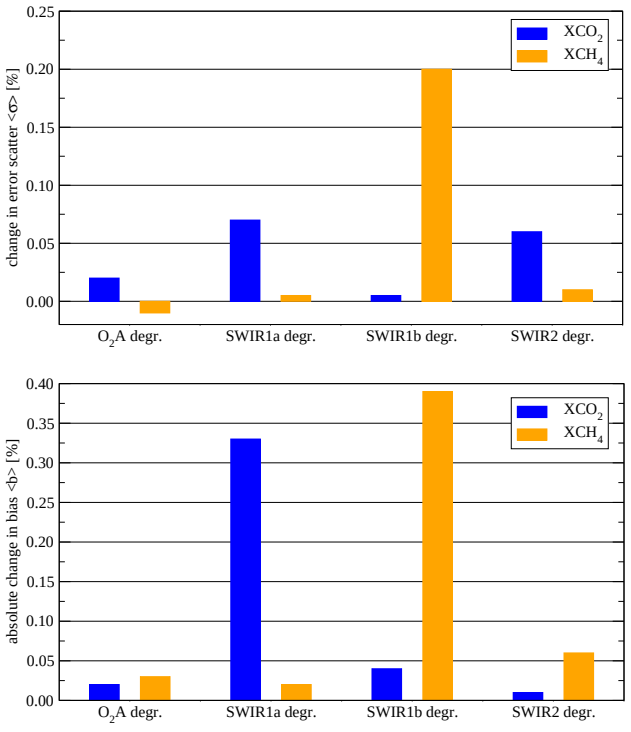

Fig. 6. Results for spectral degradation of single windows from GOSAT to 1.5 cm^{-1} resolution, averaged over all six TCCON stations. Upper panel: change of error scatter $\langle\sigma\rangle$ relative to results at GOSAT resolution, lower panel: absolute change of bias $\langle b\rangle$ relative to GOSAT resolution. Blue columns denote XCO_2, orange columns denote XCH_4.

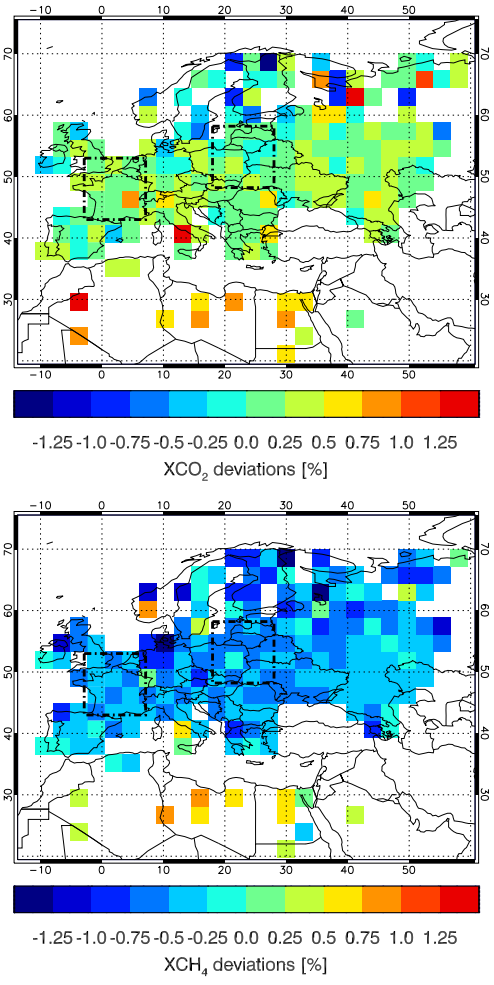

Fig. 7. Maps showing the relative differences in retrieved XCO_2 (top) and XCH_4 (bottom) between 1.5 cm^{-1} and GOSAT resolutions in Europe and northern Africa from May 2009 to May 2011. Dash-dotted squares: collocation boxes around the TCCON stations Orléans and Białystok.

they would have affected the CH_4 columns. The different effects of SWIR1a and SWIR2 on retrieved XCO_2 may be explained by the fact that only the latter contains information used to constrain scattering properties (strong absorption bands sensitive to the presence of cirrus).

3.3 Europe and northern Africa – case study for retrieval biases

In Sect. 3.1, we estimated retrieval biases with respect to water, air mass, and other parameters based on roughly 900 retrieval results, distributed over six TCCON stations. To keep the number of tables and figures reasonable, we limit ourselves in this section to the two extreme cases: GOSAT resolution and 1.5 cm^{-1} resolution. Retrieving all available GOSAT data across Europe and northern Africa from May 2009 to May 2011 increases the number of retrievals by a factor of four and it enlarges the parameter space (e.g. SZA and albedo). The improvement in geographic coverage is illustrated in Fig. 7: the dashed-dotted squares illustrate the ±5° collocation boxes around the TCCON stations Orléans and Białystok, the coloured pixels show the relative differences in percentage between GOSAT and 1.5 cm^{-1} resolutions for all filtered retrievals (top panel: XCO_2, bottom panel: XCH_4).

Table 6 gives a quantitative summary of the Europe data set with respect to scatter, global bias, and dependence on retrieval parameters. The negative shift for XCH_4 in the lower panel of Fig. 7 evaluates to −0.4 %. This confirms our findings at the six TCCON stations (cf. Tables 3 and 5). For both greenhouse gases, the standard deviation of the relative differences between the two resolutions calculates to $\sigma \approx 0.6\,\%$. The root of the square sum of this standard deviation and the one obtained for differences between GOSAT and TCCON results agrees with the scatter of the low-resolution retrievals around TCCON results (roughly 1% for both absorbers according to Tables 2 to 5). The most obvious geographic pattern in Fig. 7 is the positive bias of both absorbers above the Sahara: $\langle b\rangle = (0.7 \pm 0.1)\,\%$ for XCO_2 and

$\langle b \rangle = (0.5 \pm 0.1)$ % for XCH_4. This bias is caused by the very high albedo of these scenes (typically 0.8 at the O_2 A band). For GOSAT resolution, this bias was already demonstrated by Schepers et al. (2012) and Guerlet et al. (2013). Our study shows that this bias becomes stronger at lower resolution.

The relative change in XCO_2 and XCH_4 dependencies on physical parameters between GOSAT and 1.5 cm^{-1} resolutions follows the results obtained at the six TCCON stations (see Figs. 4, 5). Degrading the spectral resolution introduced a positive XCO_2 dependency on water and a negative XCO_2 dependency on air mass. Table 6 lists the complete results of XCO_2 and XCH_4 dependencies. XCO_2 results at lower resolution depend on water, air mass, and aerosol size parameter. XCH_4 retrieval differences correlate with water abundance.

The combination of water and air-mass dependency results in a seasonal bias of XCO_2 differences. This is demonstrated in Fig. 8. During summer, the water content of the atmosphere is high and the air mass of the observations is lower than in winter. The absence of a strong XCH_4 dependency on air mass probably explains why the seasonal XCH_4 bias is weaker. We fit a harmonic bias with a constant frequency of $\omega = 2\pi/(365 \text{ days})$. The amplitude of this bias calculates to 0.29 % for XCO_2. The 1σ probability interval of the amplitude calculates from F statistics to 0.18 %. For XCH_4, the amplitude of the seasonal bias only reaches 0.11 % and is not significant with respect to a 1σ confidence level.

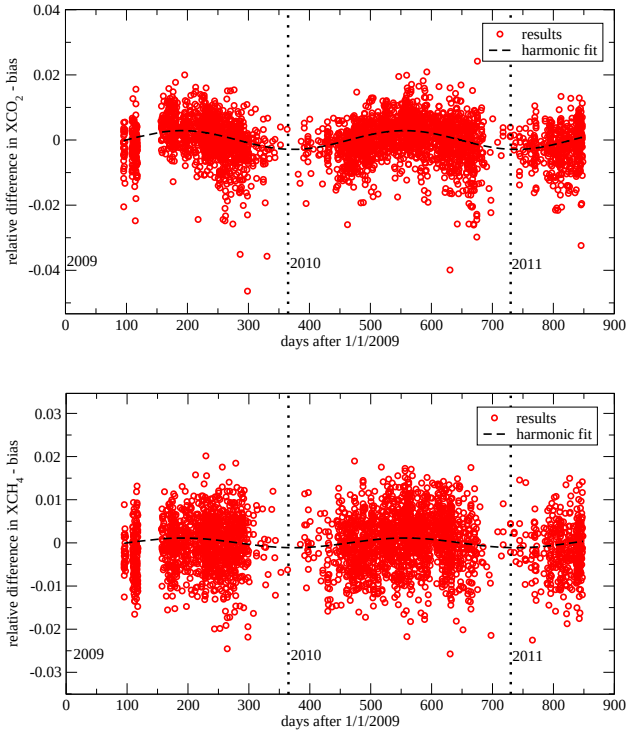

Fig. 8. Seasonal biases introduced by lowering the spectral resolution. Shown are the relative differences in retrieved XCO_2 (top) and XCH_4 (bottom) between 1.5 cm^{-1} and GOSAT resolutions for all filtered GOSAT retrievals in Europe. Amplitude of harmonic fit (black dashed lines) equals 0.0029 for CO_2 and 0.0011 for CH_4.

3.4 Synthetic spectra

To complete the examination of spectral degradation, we calculated synthetic spectra at GOSAT resolution and degraded them again to 1.5 cm^{-1} resolution. We did this for the 11 036 scenarios of the global ensemble defined by Butz et al. (2012). They cover the entire land surface at an SZA $\leq 70°$ for four days in January, April, July, and October. The synthetic scenarios include a realistic range of aerosol and cirrus optical properties. Since cirrus prefiltering (see Sect. 2.1) allows us to exclude GOSAT observations with a COT larger than 0.02, we reduced the COT of all scenarios by a factor of 10, such that 97 % have COT < 0.02. A second reason for this reduction was statistics: for nominal synthetic COT, the number of retrievals passing all filters at all resolutions and at all noise levels was not sufficient for a statistically sound statement. Reducing the COT introduced a small bias of +0.1 % for XCO_2 and +0.2 % for XCH_4.

In this section, retrieval errors represent the relative deviation of the retrieved column density of CO_2 and CH_4 from the true input column density. Contrary to real measurements, synthetic retrievals are not affected by spectroscopic errors or calibration errors. The errors that occur in synthetic retrievals originate from interference errors or from forward model errors: the treatment of scattering effects for radiative transfer in the retrieval algorithm is much simpler than the one used to simulate the measurement. The third source of errors is the noise. By default, we add Gaussian distributed noise to the calculated input spectrum; the noise amplitude is determined by the noise model. We reproduced GOSAT instrument performance assuming a SNR of 300 at the continuum and holding the absolute measurement uncertainty constant at each spectral entry. In addition, we retrieved the same synthetic spectra with reduced noise (SNR = 600) and without any noise to isolate the pure forward model and interference error in the absence of statistical errors.

The first approach with added noise is the one chosen by Butz et al. (2012) for determining the XCH_4 retrieval accuracy of a GOSAT-like instrument for a similar global ensemble. They used an earlier version of the RemoTeC algorithm with a different regularization scheme and found $\langle \sigma \rangle \approx 0.6$ % for CH_4 errors. The synthetic error scatter of CH_4 reaches only ≈ 0.4 % in the present study because of the lowered COT.

Figure 9 summarizes the retrieval accuracy of XCO_2 (cross and plus symbols) and XCH_4 (squares and circles) for synthetic scenarios. Black symbols denote GOSAT resolution, red symbols denote 1.5 cm^{-1} resolutions. In the left column, $\langle \sigma \rangle$ is shown for noiseless synthetic spectra. All four standard deviations fall between 0.2 and 0.3 %. The XCO_2 scatter increases to some extent when the spectral resolution is lowered (from 0.20 to 0.28 %); the XCH_4 scatter remains

Table 6. Impact of lowering the GOSAT spectral resolution to $1.5\,\mathrm{cm}^{-1}$ for the European data set. "Dependency" denotes the slope of a linear regression of retrieval errors against physical parameters over the entire parameter range (listed in the right column).

	XCO_2	XCH_4	Parameter range
Number of filtered retrievals	3532	3340	
Scatter σ (%)	0.64	0.62	
Bias b (%)	+0.23	−0.42	
H_2O dependency (%)	$+1.62 \pm 0.09$	$+1.20 \pm 0.09$	$(0 \ldots 2) \times 10^{23}$ mol. cm^{-2}
Air-mass dependency (%)	-1.14 ± 0.06	-0.54 ± 0.07	2.0 . . . 4.0
Albedo dependency (%)	$+0.21 \pm 0.07$	$+0.35 \pm 0.06$	0.1 . . . 0.4
Optical thickness dependency (%)	-0.03 ± 0.05	-0.25 ± 0.05	0.0 . . . 0.25
Aerosol size parameter dependency (%)	-1.85 ± 0.07	-0.45 ± 0.07	0.21 . . . 0.33

constant at 0.23 %. These small errors can be interpreted as the limit of accuracy with the present algorithm and forward model. This limit is of the same order of magnitude as the retrieval precision for GOSAT spectra. The second column shows the retrieval performance if noise is added but a very high SNR of 600 is assumed. The third column shows the synthetic retrieval results with a noise model representative to GOSAT data (SNR = 300). For this nominal synthetic scenario, we observe an increase of the error scatter when the spectral resolution is lowered: $\langle\sigma\rangle$ of XCO_2 increases from 0.40 to 0.69 %, $\langle\sigma\rangle$ of XCH_4 almost doubles from 0.42 to 0.81 %. The errors are the combination of forward model errors and statistical errors. The right column shows the retrieval accuracy found for GOSAT spectra at original and at lowered resolutions.

Contrary to the scatter, the bias of synthetic retrievals also depends on the details of the noise model, i.e. on the functional dependence of SNR with albedo, SZA, and other physical parameters. Under the assumption of a constant SNR for all synthetic observations, a negative XCH_4 bias at lower spectral resolution occurs only if noise is added to the spectra. At $1.5\,\mathrm{cm}^{-1}$, the bias reaches −0.3 % for SNR = 600 and −0.5 % for SNR = 300, whereas it remains at +0.1 % at $0.25\,\mathrm{cm}^{-1}$ resolution. This behaviour resembles real GOSAT data (see for instance Table 6). The absolute XCO_2 bias is smaller than 0.2 % for any noise level and spectral resolution.

All 12 $\langle\sigma\rangle$ values for synthetic spectra can be directly compared with each other, since we culled the results to the same total amount of 1000 filtered retrievals. The filter method was identical to the one employed for GOSAT measurements (cf. Sect. 2.1) with the following exceptions: The offset criterion was dropped because we did not introduce spectral shifts or offsets or any calibration errors when calculating input spectra. The thresholds for χ^2/DFS and $\sigma_{CO_2}, \sigma_{CH_4}$ were adapted to have the same number of filtered retrievals for all synthetic results. For a realistic noise model, χ^2/DFS typically reached 0.9 (at GOSAT resolution) instead of the 2.0 encountered for

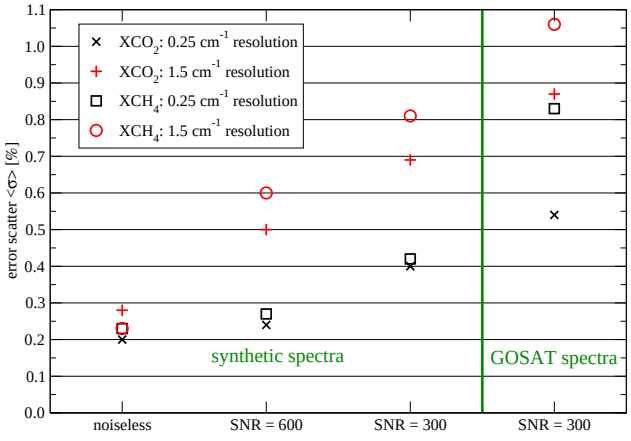

Fig. 9. Standard deviations of relative XCO_2 and XCH_4 retrieval errors for synthetic noiseless spectra (first column), for synthetic spectra with a very high SNR of 600 (second column), for synthetic spectra with nominal noise (third column), and for GOSAT spectra collocated at TCCON stations (fourth column).

GOSAT spectra. This increase of the fit residuals by a factor of two is likely caused by spectroscopic errors.

We interpret the results shown in Fig. 9 as follows: if spectroscopic errors are absent, and a perfect instrument were available, retrieval accuracy does not notably depend on spectral resolution. If spectroscopic errors are still absent but a realistic noise level is introduced, lowering spectral resolution leads to a notable increase of scatter for both XCO_2 and XCH_4. With less spectral entries, the inversion problem becomes more under-determined than at GOSAT resolution, which increases retrieval errors. The magnitude of this effect depends on spectral resolution but also on the SNR. The smaller the noise amplitude added to the spectra, the lower the retrieval errors. The relative increase of error scatter with spectral resolution also depended on the filtering criteria, but we found a relative increase of at least 30 % for both absorbers. However, we observed no significant increase of

error dependency on physical parameters when we compared synthetic retrievals of the same resolution with and without noise.

A subset of synthetic spectra with very few scatterers (optical thickness below 0.05) shows a similar relative decrease of retrieval accuracy for lower spectral resolution. For XCH_4 and SNR = 300, the scatter increases from 0.26 to 0.47 % (instead of 0.42–0.81 %) and the bias shifts by −0.5 %. For XCO_2 and SNR = 300, the scatter increases from 0.23 to 0.44 %. This loss of retrieval accuracy must be attributed to interference errors because forward model errors related to scattering are of minor importance for this subset.

Comparing synthetic retrieval results to GOSAT spectra (right column in Fig. 9) reveals a further increase of error scatter for all four cases. The strongest effect is seen for XCH_4 at high resolution: its retrieval accuracy is two times better in the synthetic case, i.e. 0.42 versus 0.83 %. It is intriguing to interpret this increase as the effect of spectroscopic and calibration errors. We caution the reader, however, that comparison of simulated and real measurements might be misleading, because the synthetic ensemble represents the entire land surface at all seasons, whereas GOSAT measurements collocated at TCCON stations represent only a small fraction of the world (Guerlet et al., 2013). If, for instance, the synthetic retrievals are reduced to scenes with albedo values between 0.1 and 0.35 – representing the span of albedo values encountered at TCCON stations – then $\langle\sigma\rangle = 0.34$ and 0.58 % instead of 0.42 and 0.81 % for XCH_4 with default SNR = 300. This would imply a larger contribution of spectroscopic and calibration errors to the total error of GOSAT retrievals than suggested by Fig. 9.

4 Conclusions

We have studied how a lower spectral resolution of satellite observations affects retrieval accuracy of CO_2 and CH_4. Since high spectral resolution is a cost driver for a satellite mission, we also wanted to check if a resulting loss in retrieval accuracy could be mitigated by a higher SNR. To address these goals, we relied on GOSAT measurements and simulated spectra at various spectral resolutions between 0.24 and 1.5 cm^{-1} to cover the range envisaged for future satellite missions.

For a given resolution of the degraded spectrum, the convolution approach with an oversampling ratio of 2.5 and the truncation approach with an oversampling ratio of 1.0 yield a similar increase in scatter and decrease of correlation. The particular shape of the ILS and the oversampling ratio are thus of minor relevance compared to the retrieval errors introduced by a reduced spectral resolution.

For CO_2 retrieval performance, the continuous increase of error scatter from $\langle\sigma\rangle = 0.65$ to 0.97 % is the most notable effect of lowering the spectral resolution step by step from 0.24 to 1.5 cm^{-1}. This increase is the net result of several dependencies on physical parameters (water, air mass, and albedo). The inter-station bias between six TCCON sites increases from 0.2 to 0.3 %. The convergence rate decreases by up to 25 %, but this figure depends on the assumed measurement uncertainty. The standard deviation of CH_4 retrieval errors increases from 0.85 to 1.03 % and the average bias drops by 0.4 % as the resolution is lowered from 0.24 to 1.5 cm^{-1}. The increase of error scatter, the bias shift and the dependency on physical parameters are also reproduced for 2 consecutive years of GOSAT measurements across Europe and northern Africa.

Degrading single windows has shown that an increase of error scatter and bias occurs only if those windows are degraded where absorption lines of the target molecules are located. Lowering the spectral resolution in regions that are only used to provide information on scatterers has little impact on retrieval accuracy. The instrument effects in the O_2 A window of GOSAT spectra (e.g. the intensity offset) do not become obviously more detrimental to accuracy at lower resolution.

The inversion of synthetic spectra demonstrates that forward model errors (introduced by the simplified aerosol model for retrieval) are much smaller than the error scatter of retrieved XCO_2 and XCH_4 established from GOSAT spectra. Moreover, lower resolution does not amplify forward model errors per se. If noise is added to the spectrum, however, the resulting interference errors become more pronounced at lower spectral resolution. Part of this increase can be considered a statistical and not a systematic error contribution. Comparison of synthetic measurements and GOSAT measurements suggests that the retrieval accuracy of CH_4 at any resolution would benefit more from a further improvement of the spectroscopy than CO_2.

Our study confirms that lowering the spectral resolution of satellite observations decreases retrieval accuracy to a certain extent for a given signal-to-noise ratio. For observations at lower spectral resolution, accurate spectroscopy of the target absorbers becomes of particular importance lest interference errors dominate the retrieval performance. A countermeasure for instruments with a lower spectral resolution than GOSAT is to aim at a higher SNR. The impact of random detector noise on retrievals with lower spectral resolution will also be smaller than presented in this paper if the loss in spectral resolution can be traded against additional measurements of the same area over a given time period.

Acknowledgements. The first author was supported by ESA under ESA contract number 4000105676/12/NL/AF. S. Guerlet acknowledges funding from ESA's Climate Change Initiative on greenhouse gases and the European Commission's Seventh Framework Programme under grant agreement 218793. A. Butz is supported by Deutsche Forschungsgemeinschaft (DFG) through the Emmy Noether Programme, grant BU2599/1-1 (RemoTeC). US funding for TCCON comes from NASA's Terrestrial Ecology Program, grant number NNX11AG01G, the Orbiting Carbon

Observatory Program, the Atmospheric CO_2 Observations from Space (ACOS) Program and the DOE/ARM Program. The Darwin TCCON site was built at Caltech with funding from the OCO project, and is operated by the University of Wollongong, with travel funds for maintenance and equipment costs funded by the OCO-2 project. We acknowledge funding to support Darwin and Wollongong from the Australian Research Council, Projects LE0668470, DP0879468, DP110103118 and LP0562346. The University of Bremen acknowledges financial support of the Białystok and Orléans TCCON sites from the Senate of Bremen and EU projects IMECC, GEOmon, InGOS, and ICOS-INWIRE, as well as maintenance and logistical work provided by AeroMeteo Service (Białystok) and the RAMCES team at LSCE (Gif-sur-Yvette, France) and additional operational funding from the National Institute for Environmental Studies. ECMWF ERA Interim analyses are provided through http://data-portal.ecmwf.int/data/d/interimdaily/. TM4 modelled CH_4 and CO concentration fields have been made available through J. F. Meirink, Royal Netherlands Meteorological Institute (KNMI).

Edited by: A. Lambert

References

Basu, S., Guerlet, S., Butz, A., Houweling, S., Hasekamp, O., Aben, I., Krummel, P., Steele, P., Langenfelds, R., Torn, M., Biraud, S., Stephens, B., Andrews, A., and Worthy, D.: Global CO_2 fluxes estimated from GOSAT retrievals of total column CO_2, Atmos. Chem. Phys., 13, 8695–8717, doi:10.5194/acp-13-8695-2013, 2013.

Boesch, H., Baker, D., Connor, B., Crisp, D., and Miller, C.: Global Characterization of CO_2 Column Retrievals from Shortwave-Infrared Satellite Observations of the Orbiting Carbon Observatory-2 Mission, Remote Sens., 3, 270–304, 2011.

Bovensmann, H., Burrows, J. P., Buchwitz, M., Frerick, J., Noël, S., Rozanov, V. V., Chance, K. V., and Goede, A. P. H.: SCIAMACHY: Mission Objectives and Measurement Modes, J. Atmos. Sci., 56, 127–150, 1999.

Buchwitz, M., Reuter, M., Bovensmann, H., Pillai, D., Heymann, J., Schneising, O., Rozanov, V., Krings, T., Burrows, J. P., Boesch, H., Gerbig, C., Meijer, Y., and Löscher, A.: Carbon Monitoring Satellite (CarbonSat): assessment of atmospheric CO_2 and CH_4 retrieval errors by error parameterization, Atmos. Meas. Tech., 6, 3477–3500, doi:10.5194/amt-6-3477-2013, 2013.

Butz, A., Hasekamp, O. P., Frankenberg, C., Vidot, J., and Aben, I.: CH_4 retrievals from space-based solar backscatter measurements: performance evaluation against simulated aerosol and cirrus loaded scenes, J. Geophys. Res., 115, D24302, doi:10.1029/2010JD014514, 2010.

Butz, A., Guerlet, S., Hasekamp, O., Schepers, D., Galli, A., Aben, I., Frankenberg, C., Hartmann, J.-M., Tran, H., Kuze, A., Keppel-Aleks, G., Toon, G., Wunch, D., Wennberg, P., Deutscher, N. M., Griffith, D., Macatangay, R., Messerschmidt, J., Notholt, J., and Warneke, T.: Toward accurate CO_2 and CH_4 observations from GOSAT, Geophys. Res. Lett., 38, L14812, doi:10.1029/2011GL047888, 2011.

Butz, A., Galli, A., Hasekamp, O., Landgraf, J., Tol, P., and Aben, I.: TROPOMI aboard Precursor Sentinel-5 Precursor: Prospective performance of CH_4 retrievals for aerosol and cirrus loaded atmospheres, Remote Sens. Environ., 120, 267–276, doi:10.1016/j.rse.2011.05.030, 2012.

Galli, A., Butz, A., Scheepmaker, R. A., Hasekamp, O., Landgraf, J., Tol, P., Wunch, D., Deutscher, N. M., Toon, G. C., Wennberg, P. O., Griffith, D. W. T., and Aben, I.: CH_4, CO, and H_2O spectroscopy for the Sentinel-5 Precursor mission: an assessment with the Total Carbon Column Observing Network measurements, Atmos. Meas. Tech., 5, 1387–1398, doi:10.5194/amt-5-1387-2012, 2012.

Guerlet, S., Butz, A., Schepers, D., Basu, S., Hasekamp, O. P., Kuze, A., Yokota, T., Blavier, J.-F., Deutscher, N. M., Griffith, D. W. T., Hase, F., Kyrö, E., Morino, I., Sherlock, V., Sussmann, R., Galli, A., and Aben, I.: Impact of aerosol and thin cirrus on retrieving and validating XCO_2 from GOSAT shortwave infrared measurements, J. Geophys. Res.-Atmos., 118, 4887–4905, doi:10.1002/jgrd.50332, 2013.

Hasekamp, O. P. and Butz, A.: Efficient calculation of intensity and polarization spectra in vertically inhomogeneous scattering and absorbing atmospheres, J. Geophys. Res., 113, D20309, doi:10.1029/2008JD010379, 2008.

Ingmann, P., Veihelmann, B., Langen, J., Lamarre, D., Stark, H., and Courrèges-Lacoste, G. B.: Requirements for the GMES Atmosphere Service and ESA's implementation concept: Sentinels-4/-5 and -5p, Remote Sens., 120, 58–69, 2012.

Kuze, A., Suto, H., Nakajima, M., and Hamazaki, T.: Thermal and near infrared sensor for carbon observation Fourier-transform spectrometer on the Greenhouse Gases Observing Satellite for greenhouse gases monitoring, Appl. Optics, 48, 6716, doi:10.1364/AO.48.006716, 2009.

Lamouroux, J., Tran, H., Laraia, A. L., Gamache, R. R., Rothman, L. S., Gordon, I. E., and Hartmann, J.-M.: Updated database plus software for line-mixing in CO_2 infrared spectra and their test using laboratory spectra in the 1.5–2.3 µm region, J. Quant. Spectrosc. Ra., 111, 2321–2331, 2010.

Liu, Y., Yang, D. X., and Cai, Z. N.: A retrieval algorithm for TanSat XCO_2 observation: Retrieval experiments using GOSAT data, Chinese Sci. Bull., 58, 1520–1523, doi:10.1007/s11434-013-5680-y, 2013.

Morino, I., Uchino, O., Inoue, M., Yoshida, Y., Yokota, T., Wennberg, P. O., Toon, G. C., Wunch, D., Roehl, C. M., Notholt, J., Warneke, T., Messerschmidt, J., Griffith, D. W. T., Deutscher, N. M., Sherlock, V., Connor, B., Robinson, J., Sussmann, R., and Rettinger, M.: Preliminary validation of column-averaged volume mixing ratios of carbon dioxide and methane retrieved from GOSAT short-wavelength infrared spectra, Atmos. Meas. Tech., 4, 1061–1076, doi:10.5194/amt-4-1061-2011, 2011.

Oshchepkov, S., Bril, A., Yokota, T., Wennberg, P. O., Deutscher, N. M., Wunch, D., Toon, G. C., Yoshida, Y., O'Dell, C. W., Crisp, D., Miller, C. E., Frankenberg, C., Butz, A., Aben, J., Guerlet, S., Hasekamp, O., Boesch, H., Cogan, A., Parker, R., Griffith, D., Macatangay, R., Notholt, J., Sussmann, R., Rettinger, M., Sherlock, V., Robinson, J., Kyrö, E., Heikkinen, P., Feist, D. G., Morino, I., Kadygrov, N., Belikov, D., Maksyutov, S., Matsunaga, T., Uchino, O., and Watanabe, H.: Effects of atmospheric light scattering on spectroscopic observations of greenhouse gases from space. Part 2: Algorithm intercomparison in the GOSAT data processing for CO_2 retrievals over TCCON sites, J. Geophys. Res.-Atmos., 118, 1493–1512, doi:10.1002/jgrd.50146, 2013.

Parker, R., Boesch, H., Cogan, A., Fraser, A., Feng, L., Palmer, P. I., Messerschmidt, J., Deutscher, N. M., Griffith, D. W. T., Notholt, J., Wennberg, P. O., and Wunch, D.: Methane observations from the Greenhouse Gases Observing SATellite: Comparison to ground-based TCCON data and model calculations, Geophys. Res. Lett., 38, 2–7, doi:10.1029/2011GL047871, 2011.

Petri, C., Warneke, T., Jones, N., Ridder, T., Messerschmidt, J., Weinzierl, T., Geibel, M., and Notholt, J.: Remote sensing of CO_2 and CH_4 using solar absorption spectrometry with a low resolution spectrometer, Atmos. Meas. Tech., 5, 1627–1635, doi:10.5194/amt-5-1627-2012, 2012.

Reuter, M., Bovensmann, H., Buchwitz, M., Burrows, J. P., Connor, B. J., Deutscher, N. M., Griffith, D. W. T., Heymann, J., Keppel-Aleks, G., Messerschmidt, J., Notholt, J., Petri, C., Robinson, J., Schneising, O., Sherlock, V. Velazco, V., Warneke, T., Wennberg, P. O., and Wunch, D.: Retrieval of atmospheric CO_2 with enhanced accuracy and precision from SCIAMACHY: Validation with FTS measurements and comparison with model results, J. Geophys. Res., 116, D04301, doi:10.1029/2010JD015047, 2011.

Rothman, L. S., Gordon, I. E., Barbe, A., Benner, D. C., Bernath, P. F., Birk, M., Boudon, V., Brown, L. R., Campargue, A., Champion, J., Chance, K., Coudert, L. H., Dana, V., Devi, V. M., Fally, S., Flaud, J., Gamache, R. R., Goldman, A., Jacquemart, D., Kleiner, I., Lacome, N., Lafferty, W. J., Mandin, J., Massie, S. T., Mikhailenko, S. N., Miller, C. E., Moazzen-Ahmadi, N., Naumenko, O. V., Nikitin, A. V., Orphal, J., Perevalov, V. I., Perrin, A., Predoi-Cross, A., Rinsland, C. P., Rotger, M., Šimečková, M., Smith, M. A. H., Sung, K., Tashkun, S. A., Tennyson, J., Toth, R. A., Vandaele, A. C., and Vander Auwera, J.: The HITRAN 2008 molecular spectroscopic database, J. Quant. Spectrosc. Ra., 110, 533–572, 2009.

Schepers, D., Guerlet, S., Butz, A., Landgraf, J., Frankenberg, C., Hasekamp, O., Blavier, J.-F., Deutscher, N. M., Griffith, D. W. T., Hase, F., Kyrö, E., Morino, I., Sherlock, V., Sussmann, R., and Aben, I.: Methane retrievals from Greenhouse Gases Observing Satellite (GOSAT) shortwave infrared measurements: Performance comparison of proxy and physics retrieval algorithms, J. Geophys. Res., 117, D10307, doi:10.1029/2012JD017549, 2012.

Sussmann, R. and Borsdorff, T.: Technical Note: Interference errors in infrared remote sounding of the atmosphere, Atmos. Chem. Phys., 7, 3537–3557, doi:10.5194/acp-7-3537-2007, 2007.

Tran, H. and Hartmann, J.-M.: An improved O_2 A-band absorption model and its consequences for retrievals of photon paths and surface pressures, J. Geophys. Res., 113, D18104, doi:10.1029/2008JD010011, 2008.

Wunch, D., Toon, G. C., Wennberg, P. O., Wofsy, S. C., Stephens, B. B., Fischer, M. L., Uchino, O., Abshire, J. B., Bernath, P., Biraud, S. C., Blavier, J.-F. L., Boone, C., Bowman, K. P., Browell, E. V., Campos, T., Connor, B. J., Daube, B. C., Deutscher, N. M., Diao, M., Elkins, J. W., Gerbig, C., Gottlieb, E., Griffith, D. W. T., Hurst, D. F., Jiménez, R., Keppel-Aleks, G., Kort, E. A., Macatangay, R., Machida, T., Matsueda, H., Moore, F., Morino, I., Park, S., Robinson, J., Roehl, C. M., Sawa, Y., Sherlock, V., Sweeney, C., Tanaka, T., and Zondlo, M. A.: Calibration of the Total Carbon Column Observing Network using aircraft profile data, Atmos. Meas. Tech., 3, 1351–1362, doi:10.5194/amt-3-1351-2010, 2010.

Wunch, D., Toon, G. C., Blavier, J.-F. L., Washenfelder, R. A., Notholt, J., Connor, B. J., Griffith, D. W. T., Sherlock, V., and Wennberg, P. O.: The Total Carbon Column Observing Network, Phil. Trans. R. Soc. A, 369, 2087–2112, doi:10.1098/rsta.2010.0240, 2011a.

Wunch, D., Wennberg, P. O., Toon, G. C., Connor, B. J., Fisher, B., Osterman, G. B., Frankenberg, C., Mandrake, L., O'Dell, C., Ahonen, P., Biraud, S. C., Castano, R., Cressie, N., Crisp, D., Deutscher, N. M., Eldering, A., Fisher, M. L., Griffith, D. W. T., Gunson, M., Heikkinen, P., Keppel-Aleks, G., Kyrö, E., Lindenmaier, R., Macatangay, R., Mendonca, J., Messerschmidt, J., Miller, C. E., Morino, I., Notholt, J., Oyafuso, F. A., Rettinger, M., Robinson, J., Roehl, C. M., Salawitch, R. J., Sherlock, V., Strong, K., Sussmann, R., Tanaka, T., Thompson, D. R., Uchino, O., Warneke, T., and Wofsy, S. C.: A method for evaluating bias in global measurements of CO_2 total columns from space, Atmos. Chem. Phys., 11, 12317–12337, doi:10.5194/acp-11-12317-2011, 2011b.